Building Engineering 2025, 3(2), 2207.
https://doi.org/10.59400/be2207

Article

CFD-based comparative simulation analysis of flow field under different natural ventilation boundary conditions in the room

Yuanyuan Fu*, Bin Zhao

School of Mechanical Engineering, Liaoning Petrochemical University, Fushun 113001, China
*** Corresponding author:** Yuanyuan Fu, 1500539857@qq.com

CITATION

Fu Y, Zhao B. CFD-based comparative simulation analysis of flow field under different natural ventilation boundary conditions in the room. Building Engineering. 2025; 3(2): 2207. https://doi.org/10.59400/be2207

ARTICLE INFO

Received: 4 December 2024
Accepted: 13 February 2025
Available online: 10 April 2025

Abstract: In order to achieve reasonable indoor layout design, reduce building energy consumption and better meet human body thermal comfort requirements, flow fields under different natural ventilation conditions are compared based on computational fluid dynamics (CFD) in this paper. Firstly, a theoretical model of the indoor flow field under six different ventilation conditions is constructed, and boundary conditions, wall functions and meshing structure are confirmed. Simulation analysis is carried out for six different working conditions. Through comparative analysis, it is concluded the window opening location should be located in the center, and the direct airflow through the convection field is evenly distributed, and the direct airflow is conducive to the improvement of indoor cleanliness. In addition, when organizing natural ventilation, the window orientation is inclined to the dominant wind direction in summer by about 45° angles, it can improve the ventilation effect. And by analyzing temperature contours, 45° angles can better meet people's needs about temperature: 18 ℃–26 ℃. When temperature contours' temperature is above people's comfortable temperature in specific rooms or places, mechanical ventilation and evaporative cooling can be combined. Research results can not only significantly improve the quality of living and working environments, but also help promote the development of green buildings and achieve energy-saving and emission reduction goals.

Keywords: natural ventilation; thermal comfort; building energy conservation; reasonable indoor arrangement

1. Introduction

With the development of the economy, Internet technology is becoming more and more developed, which provides the possibility of working at home. More people choose to work at home, so people have higher requirements for indoor thermal comfortable environments. According to statistics, people generally stay in buildings for over 90% of their time, which occupies 40% of anthropogenic greenhouse gas emissions and is a main decider of weather differences. Incentivizing more durable buildings, building codes can be applied in strengthening indoor comfort levels and least energy efficiency needs [1]. Meanwhile, energy consumption is also a problem that cannot be ignored all over the world. Therefore, more and more scholars focus on not only meeting the human body's thermal comfort but also pursuing reduced energy consumption.

Natural ventilation is a very sensitive energy efficiency protection means, and sufficient climatic categorization with regard to construction is a fundamental and essential step toward building potential evaluation [2]. Application of natural ventilation for cooling in summer can positively improve the indoor thermal

environment and thermal comfort [3]. Especially in summer, natural ventilation is conducive to decreasing indoor temperature and lowering indoor air's concentration of pollutants under high temperatures, thereby improving indoor gas quality and reducing energy depletion. What's more, natural ventilation is applied to decrease residential energy depletion and carbon release, decreasing the requirement for mechanical ventilation [4]. Therefore, natural ventilation as a way to not consume any non-renewable energy can effectively improve indoor temperature, humidity and improve the indoor environment, which is conducive to people's physical and mental health, and better improves the efficiency of work and study.

So far, some scientists have been concerned about indoor natural ventilation, and some excellent achievements have been obtained. Hsu et al. [5] employed response surface methodology, back-propagation neural networks, and multiple linear regression to investigate different factors' effects on natural ventilation. Experiments were conducted in classrooms facing non-windward directions, measuring indoor air changes per hour (ACH) during peak noon temperatures. Thermal comfort was evaluated by using predicted mean vote (PMV). The experimental results showed that single window openings provided better thermal comfort compared to cross window openings while maintaining indoor CO_2 concentrations below 1000 ppm. Furthermore, subsequent analysis revealed that the opening size (open and open/gap) increases the range of ACH, suggesting avenues for future research to enhance natural ventilation practices. This underscores natural ventilation's potential in maintaining indoor thermal comfort and CO_2 levels under challenging conditions.

Zhang et al. [6] analyzed a building for a science museum considering atrium-centered natural ventilation. Floor design, building direction, and inside construction are designed to effectively use natural ventilation for decreasing space temperature under local climatic status. The natural ventilation model is constructed through computational fluid dynamics for gas flow assessment. Results show that novel building designs could obtain better effects. Iskandar et al. [7] compared different natural ventilation means through simulation analysis, and results were discussed. Results showed that considered conditions could be a benefit for energy savings for different seasons. It also showed that the size of openings had an effect on thermal comfort. This research showed that historic preservation and thermal comfort aims could be obtained at the same time.

Kocik et al. [8] analyzed three models based on simulation: predicted mean vote, thermal sensation model, and advanced dynamic thermal sensation model, which allowed demonstration of differences in thermal comfort evaluation. Analysis results had shown that opening the window with the door closed had a negligible effect on indoor environment parameters. Effect increased during autumn and winter, which decides thermal sensations. Cheng et al. [9] applied a four-student dormitory as a research object. Volume ratios of air age curves are established according to air age values. Due to the symmetry of the dormitory, five wind angles, averaged from 0 degrees to 90 degrees, were selected. Results showed that average indoor air temperature can be stabilized above 11 degrees in rooms located on the leeward side of the dormitory. Nguyen et al. [10] proposed a novel CFD method that was applied over set grids to evaluate natural ventilation. The proposed model is firstly verified by different measurements from literature for wind flow predictions before being applied

for design exploration in high-rise residential. Ventilation metrics were also analyzed for different parameters. This research showed the merits of the proposed approach for natural ventilation.

Wang et al. [11] applied a full-size simulation means to study the influence of no deflector, deflectors with different opening width-to-height ratios and deflectors with different opening shapes on the percentage of indoor velocity partitions. Results showed that judicious installation of deflectors could increase indoor airflow velocity distribution and enhance the percentage of indoor comfort zones. Nasrollahi et al. [12] applied two means of field studies and simulation modeling to enhance high-rise thermal comfort. Results of current research showed that although cooling energy needs in high-rise buildings in hot climates were high and application of natural ventilation systems was beneficial. Tian et al. [13] applied two means of simulations and orthogonal design to study different building opening factors' influence on indoor thermal comfort. Results showed that vortices could lead to poor ventilation, but indoor circulation could increase air exchange efficiency.

This research takes a room as a research object, and uses computational fluid dynamics to simulate and analyze indoor flow fields under different natural ventilation conditions to provide a favorable theoretical basis for improvement of indoor comfort. Based on the above study on indoor natural ventilation, the author also aimed at the clover house layout, under different boundary conditions, such as different inlet air angles and entrance windows' number and positions. Through comparative analysis, it was obtained where the ventilation effect was the best, and the human body's thermal comfort could be achieved only by relying on natural ventilation. Where the ventilation effect is second, it is necessary to install electric fans, air conditioners, and other equipment for mechanical ventilation. It is conducive to building energy savings and reducing energy consumption.

This study aims to use CFD simulations to gain a deeper understanding of how wind pressure and thermal pressure affect indoor ventilation effectiveness under different conditions, as well as their interrelationships. By comparing the flow field simulation results under different natural ventilation boundary conditions, the optimal ventilation design scheme is identified to improve indoor ventilation efficiency and quality.

2. Physical mathematical model of indoor flow field

Reynolds-averaged Navier-Stokes equations are applied to analyze turbulent flow because they can effectively describe physical quantities' statistical average and other statistical randomness in turbulence. Due to the standard k-ε model having good convergence and low memory usage, it can be applied in exterior flow with complex geometries as well as non-slip wall flow [14]. Therefore, the standard k-ε model can be applied to analyze Reynolds stress. ANSYS Fluent has four types of wall functions, standard wall function, scalable wall function, non-equilibrium wall function and enhanced wall function respectively [15]. For medium-density meshes, the standard wall function not only has the best adaptability to the mesh and flow but also has the best prediction ability. Standard Wall Functions is Fluent software's default option, which is suitable for high Reynolds number flows. It has a wide range of industry

applications, suitable for situations near the wall flow's little impact on the study's problem, but is not suitable for large pressure gradients.

The mathematical model formulas of the indoor flow field are listed as follows:

(1) The standard *k*-*ε* model's relevant formula

The basic governing equations of the standard turbulence model are as follows:

The mass conservation equation is listed as follows:

$$\frac{\partial \rho}{\partial t} + u\frac{\partial(\rho u)}{\partial x} + v\frac{\partial(\rho v)}{\partial y} + w\frac{\partial(\rho w)}{\partial z} = 0 \tag{1}$$

Momentum conservation equations are listed as follows:

$$\begin{aligned} \rho\frac{\partial u}{\partial t} &= \rho F_{bx} + \frac{\partial p_{xx}}{\partial x} + \frac{\partial p_{yx}}{\partial y} + \frac{\partial p_{zx}}{\partial z} \\ \rho\frac{\partial v}{\partial t} &= \rho F_{by} + \frac{\partial p_{xy}}{\partial x} + \frac{\partial p_{yy}}{\partial y} + \frac{\partial p_{zy}}{\partial z} \\ \rho\frac{\partial w}{\partial t} &= \rho F_{bz} + \frac{\partial p_{xz}}{\partial x} + \frac{\partial p_{yz}}{\partial y} + \frac{\partial p_{zz}}{\partial z} \end{aligned} \tag{2}$$

The energy equation is listed as follows:

$$\frac{\partial}{\partial t}(\rho E) + \frac{\partial}{\partial x_i}[u_i(\rho E + P)] = \frac{\partial}{\partial x_i}\left[k_{eff}\frac{\partial t}{\partial x_i} - \sum_j h_j J_j + u_j(\tau_{ij})\right] + S_h \tag{3}$$

where, $\mathrm{E} = \mathrm{H} - \frac{p}{\rho} + \frac{u_i^2}{2}$

According to the fact that the indoor airflow in buildings is generally incompressible and low-velocity turbulent [16], this research objective uses the standard *k*-*ε* turbulence model of incompressible gas in Fluent, where the *k* equation and the *ε* equation can be simplified as follows:

$$\rho\frac{Dk}{D_t} = \frac{\partial}{\partial x_i}\left[\left(\mu + \frac{\mu_t}{\sigma_k}\right)\frac{\partial k}{\partial x_i}\right] + G_k - \rho\varepsilon \tag{4}$$

$$\rho\frac{D\varepsilon}{D_t} = \frac{\partial}{\partial x_i}\left[\left(\mu + \frac{\mu_t}{\sigma_\varepsilon}\right)\frac{\partial \varepsilon}{\partial x_i}\right] + C_{1\varepsilon}\frac{\varepsilon}{k}G_k - C_{2\varepsilon}\rho\frac{\varepsilon^2}{k} \tag{5}$$

The turbulent viscosity coefficient is expressed by

$$\mu_t = \rho C_\mu \frac{k^2}{\varepsilon} \tag{6}$$

In the formula, ρ is fluid density; μ_t is a component of the fluid in the *t*-direction; G_k represents turbulent energy due to the average velocity gradient; $C_{1\varepsilon}$ and $C_{2\varepsilon}$ are constant; $C_{1\varepsilon}$ = 1.44, $C_{2\varepsilon}$ = 1.92; σ_k and σ_ε are turbulence number, σ_k = 1.0, σ_ε = 1.3. C_μ = 0.09 is empirical coefficient, ε is turbulence dissipation rate.

Among them, the standard wall function method first defines the dimensionless parameters, including dimensionless velocity, dimensionless distance and dimensionless temperature.

Dimensionless velocity:

$$u^+ = \rho u_0 (C_\mu^{\frac{1}{4}} k_0^{\frac{1}{2}})/\tau_w \tag{7}$$

Dimensionless distance:

$$y^+ = \rho y_0 (C_\mu^{\frac{1}{4}} k_0^{\frac{1}{2}})/\mu \tag{8}$$

Dimensionless temperature:

$$T^+ = \rho C_p (T_0 - T_w)(C_\mu^{\frac{1}{4}} k_0^{\frac{1}{2}})/q_w \tag{9}$$

where, u_0 represents the velocity of the first node near the wall, y_0 is the distance from the node to the wall surface near the wall, k_0 is the turbulent energy of the node, T_0 is the temperature of the node, μ is hydrodynamic viscosity, C_p is fluid heat capacity, τ_w is wall viscosity coefficient, T_w is the wall temperature, and q_w is the heat flow.

3. Model construction of indoor flow field

(1) Simulation model

The indoor 2D simplified model is shown in **Figure 1**. In **Figure 1**, the numbers 1, 2, 3, 4, 5, 6, and 7 are used to represent the window opening's position, the number 8 represents the door's position. And the letters *A*, *B*, *C*, *D*, *E*, *F*, *G*, and *H* represent different rooms.

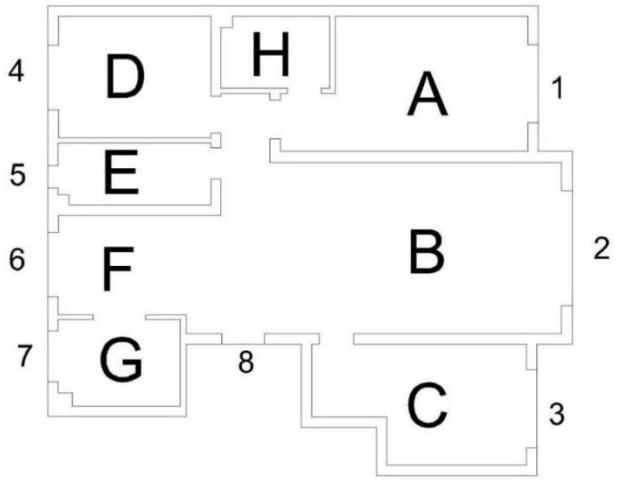

Figure 1. Indoor 2D simplified model with number.

(2) Boundary condition setting

The theoretical model of the boundary is as follows:

(a) Inlet boundary condition: due to the influence of surface friction, outdoor wind speed above the ground increases with the height, and the wind speed below 300 m can be determined according to the average wind speed gradient, and the wind speed's change rule along the height can be described by the exponential equation:

$$v(z) = v(z_0)(\frac{z}{z_0})(\frac{z}{z_0})^\alpha \tag{10}$$

In the formula, $v(z)$ is wind speed at the height of z-above ground, m/s; $V(z_0)$ is wind speed at reference z_0, m/s.

(b) Outlet boundary condition: Assuming that the fluid is fully developed, the boundary condition is the free exit boundary (outflow).

Therefore, in this case, the inlet flow velocity is 3 m/s, the inlet temperature is 20 ℃ and the inlet wind speed direction has a vertical window entering at 30°, 45° and 60°. Thickness of wall and door is 0.1 m, and thermal conductivity is 0.02 W/m^3. And the interior wall's temperature is 28 ℃, the door temperature is 26 ℃, the exterior wall's temperature is 24 ℃ and the indoor temperature is 31 ℃. The detailed boundary conditions' data is shown in **Table 1**.

Table 1. Boundary conditions for simulation.

Item	**Boundary Condition Setting**
Inlet	Temperature: 20 ℃ Velocity: 3 m/s
Outlet	Outflow
Door	(1) temperature is 26 ℃, (2) wall thickness is 0.1 m. (3) thermal conductivity is 0.02 W/m^3.
Initial room temperature	The temperature is 31 ℃.
Wall	Interior wall: (1) temperature is 28 ℃, (2) wall thickness is 0.1 m. (3) thermal conductivity is 0.02 W/m^3. Exterior wall: (1) temperature is 24 ℃, (2) wall thickness is 0.1 m. (3) thermal conductivity is 0.02 W/m^3.
Wall Function	Standard Wall Function
Turbulence Model	Standard k-ε model
Other parameters	Fluent software's default value

(3) Meshing structure model

The meshes of CFD models are divided into two categories: structured meshes and unstructured meshes. Unstructured meshes include a variety of forms, such as triangles, tetrahedrals, squares and hexahedrons. Unstructured meshes are highly adaptable to fluid computing conditions with irregular contours or local fluids that need to be encrypted and accurately calculated. While the topology of the structured mesh is strictly ordered, with the highest calculation accuracy and fast generation speed [17]. Therefore, a structured mesh is used for the indoor natural ventilation heat transfer simulation's meshing. What's more, for the paper's 2D indoor model, triangular and quadrilateral meshes are included.

To exclude the effect of the number of mesh cells in the computational zone on analysis results, a grid independence verification was carried out with five different grid sizes. The five types of grid numbers are 2040, 2364, 2872, 3487 and 4617 respectively, as shown in **Figure 2**. **Figure 2** verifies the grid independence when the wind direction projection angle is 0°, and when the number of grids reaches 2364, the maximum flow velocity tends to be stable. Considering analysis velocity and

correctness of results, it is reasonable to use 2872 grids for discretizing the analysis zone in the simulation. Meshing quality is good and satisfies the need for simulation.

The optimal indoor 2D model's meshing is shown in **Figure 3**. As shown in **Figure 2**, a structured mesh is used for the indoor natural ventilation heat transfer simulation's meshing.

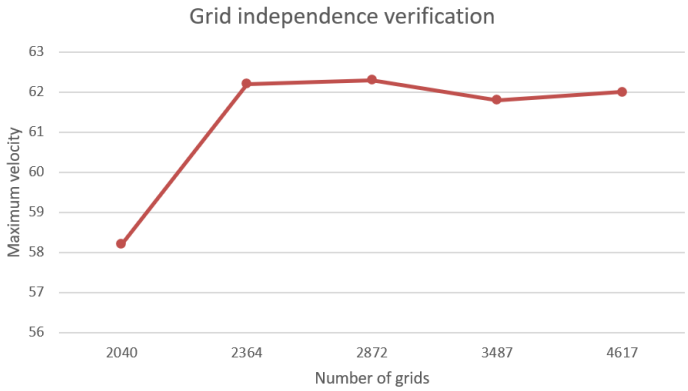

Figure 2. Grid independence verification.

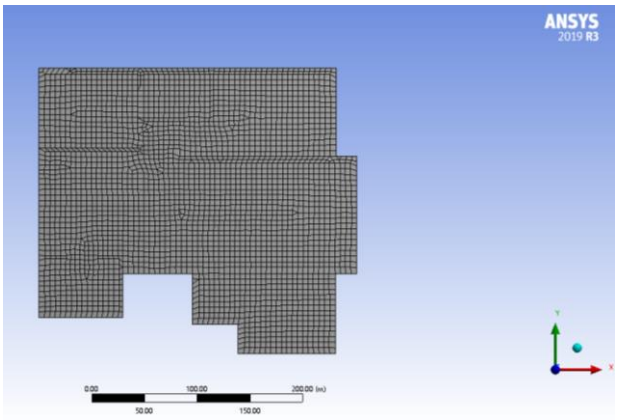

Figure 3. Meshing diagram.

(4) Working conditions

In order to effectively analyze the indoor flow field changing mechanism, six working conditions are used to carry out a comparison analysis, which is listed in **Table 2**.

Table 2. Six working conditions.

Working Condition	**Boundary conditions**
Working Condition 1	Inlet-window: number is 1, 2, 3 outlet-window: number is 4, 5, 6, 7 Wind direction projection angle: 0°
Working Condition 2	Inlet-window: number is 1, 2, 3 outlet-window: number is 4, 5, 6, 7 Wind direction projection angle: 45° downward
Working Condition 3	Inlet-window: number is 1, 2, 3 outlet-window: number is 4, 5, 6, 7 Wind direction projection angle: 45°upward

Table 2. (*Continued*).

Working Condition	Boundary conditions
Working Condition 4	Inlet-window: number is 2 outlet-window: number is 4, 5, 6, 7 Wind direction projection angle: 0°
Working Condition 5	Inlet-window: number is 2 outlet-window: number is 5, 6 Wind direction projection angle: 0°
Working Condition 6	Inlet-window: number is 3 outlet-window: number is 5, 6 Wind direction projection angle: 0°

4. Analysis of simulation results

(1) Flow field changing rules under working condition 1

The temperature contour is shown in **Figure 4**, the velocity vector diagram is shown in **Figure 5**, the pressure contour is shown in **Figure 6** and the trace diagram is shown in **Figure 7**.

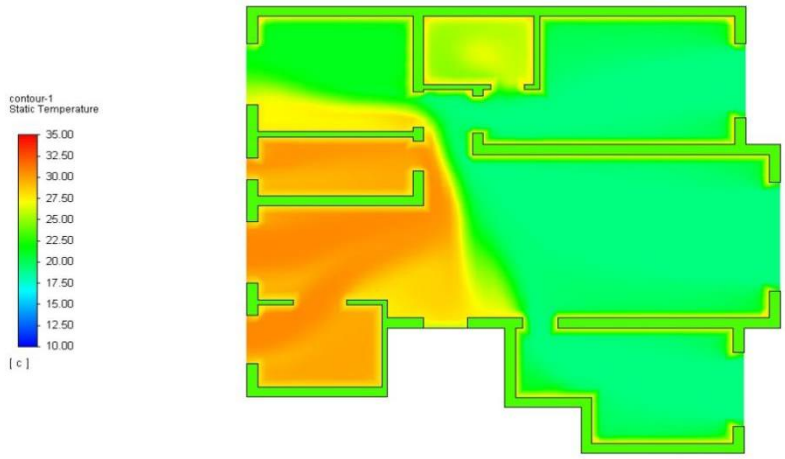

Figure 4. Temperature contour of working condition 1.

From **Figure 4**, it can be seen that the temperature of the room near the window can more easily reach the human body's thermal comfort temperature, but the EFG three rooms' temperature is relatively high. Therefore, these rooms can use the mechanical refrigeration system, such as electric fans and air conditioners. This way is more targeted and effective. In the rest of the rooms, which can meet the human body's thermal comfort only by natural ventilation, there is no need to set up a mechanical refrigeration system, which can effectively save energy and reduce energy consumption.

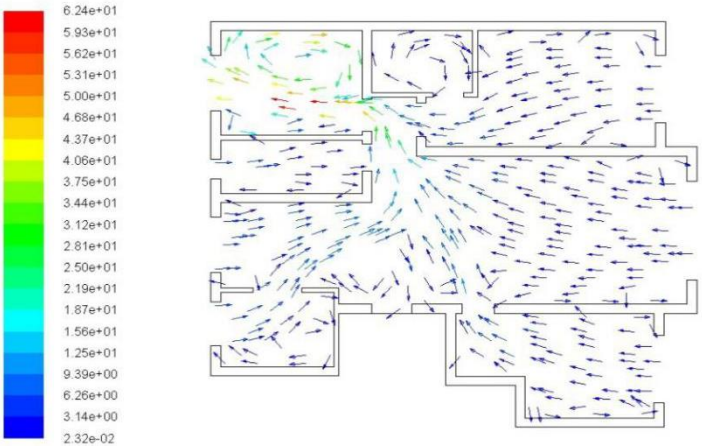

Figure 5. Velocity vector diagram of working condition 1.

From **Figure 5**, it can be seen that the flow velocity in the *D* room is large, and the air velocity's value is bound to affect the human body's comfort. When the air velocity is too high, it can increase evaporation and heat dissipation, which can make the human body feel cooler. When the air velocity is too low, the heat can't easily dissipate, and the human body can't feel comfortable. Therefore, heat dissipation equipment can be added in the low flow rate location.

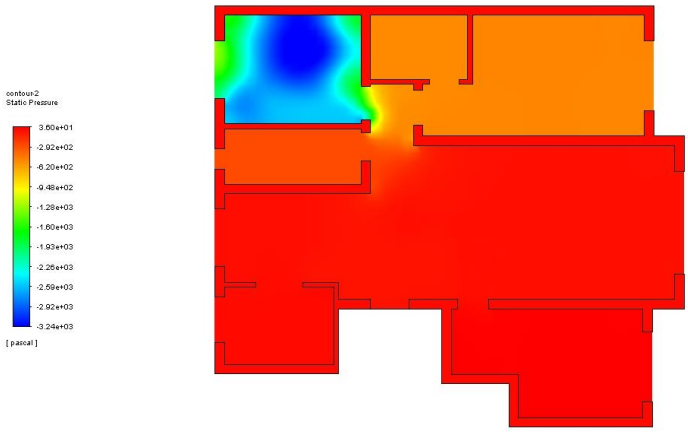

Figure 6. Pressure contour of working condition 1.

Through the comparison of the velocity vector diagram and the pressure contour diagram, it can be seen that pressure is low and flow velocity is large. As can be seen from the figure, *D* room's flow rate is larger, and *D* room's flow rate can be reduced by changing the room's internal structure in order to avoid the human body's discomfort caused by excessive blowing sensation, and then better meet the human body's velocity comfort.

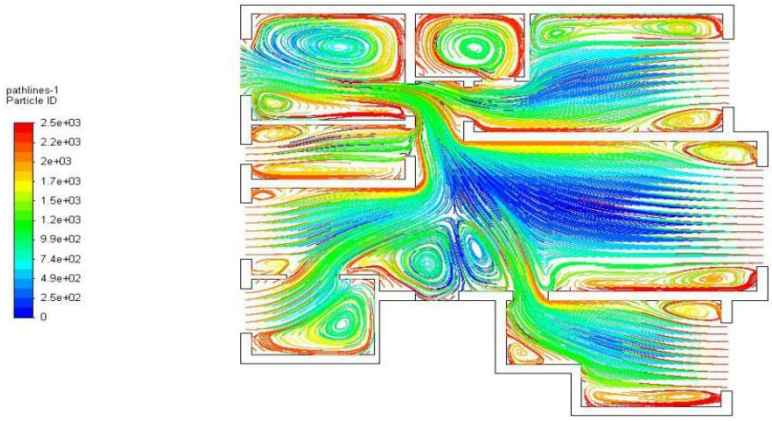

Figure 7. Trace diagram of working condition 1.

Through the **Figure 7** trace diagram, it can be seen that there are more particles and dust in the corners around the room, and the cleanliness is not good. Therefore, when people work indoors for a long time, it is better to work in a well-ventilated place, which is conducive to their health. At the same time, for industrial clean rooms that need to meet the requirements of process design, bioengineering that meets the high requirements of dust-free, such as medical, pharmaceutical, and laboratory animals, CFD simulation can be used to simulate the particle streamline diagram, and set up an excellent air filtration system at high particle concentration.

What's more, as shown in **Figure 7**, it can be seen that there are vortices of different sizes around different rooms. Vortices are manifestly the most attractive characteristics of airflow flows happening. They are highly rotating zones of airflow that often take the form of elongated filaments [18].

(2) Flow field changing rules of working condition 2.

The temperature contour of working condition 2 is shown in **Figure 8**, the velocity vector diagram of working condition 2 is shown in **Figure 9**, and the trace diagram of working condition 2 is shown in **Figure 10**.

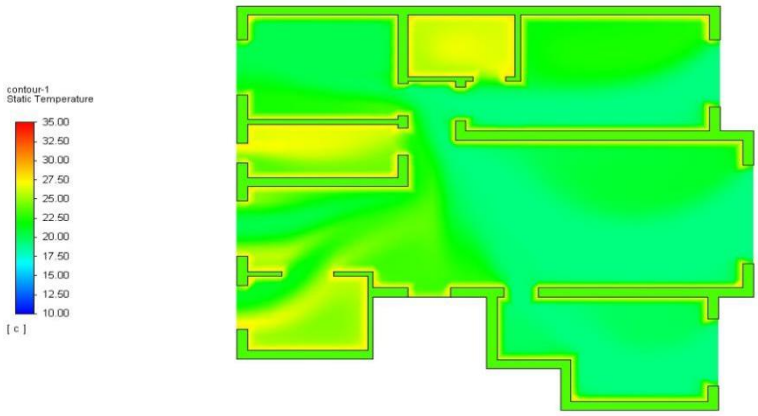

Figure 8. Temperature contour of working condition 2.

From the comparison of **Figures 4** and **8**, it can be seen that when inlet wind speed is obliquely downward by 45°, EFG's three rooms' temperature in **Figure 4** is too high, and it is necessary to set up electric fans and other equipment to achieve human comfort in the room. While in **Figure 8**, by changing the inlet wind speed's

direction, the comfortable temperature can be reached only through natural ventilation. It is more effective in energy saving than 0° the wind projection angle in **Figure 4**.

At the same time, natural ventilation has the following effective significance:

1) Low-carbon environmental sustainability, natural ventilation, can't consume any non-renewable energy, and can take away the poor-quality air and improve indoor temperature and humidity to improve the indoor environment.

2) Natural ventilation can provide fresh and clean natural air, improve indoor air composition, which is conducive to people's physiological and mental health, and then better improve people's learning and work efficiency.

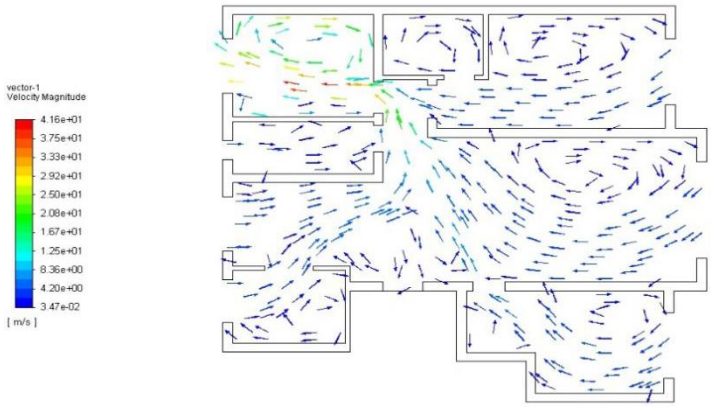

Figure 9. Velocity vector diagram of working condition 2.

Air velocity is one of the key factors affecting the indoor environment's quality, and proper air velocity can improve human comfort, but too fast air velocity may cause discomfort. In this study, the indoor environment's value is high. Therefore, the airflow rate can be appropriately increased so that the human body surface's heat can be taken away more quickly through convection. Thereby, natural ventilation can reduce the human body's thermal sensation, and then increase the human thermal comfort. At the same time, proper air velocity also helps to regulate the air's ambient humidity. When the indoor humidity is high, increasing the air flow rate can speed up the moisture discharge, reduce the indoor humidity and thus improve human comfort.

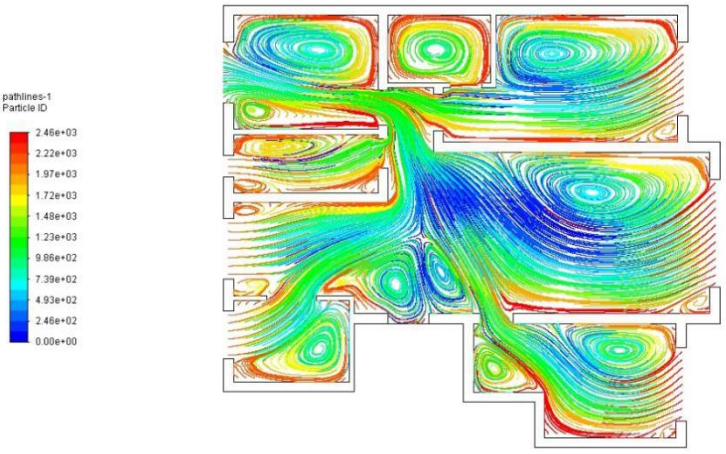

Figure 10. Trace diagram of working condition 2.

As can be seen from **Figure 10**, the particles' concentration around the room is high, and the room's cleanliness can be improved by using the above methods.

(3) Indoor flow field of working condition 3

The temperature contour of working condition 2 is shown in **Figure 11**, the trace diagram of working condition 2 is shown in **Figure 12** and the velocity vector diagram of working condition 2 is shown in **Figure 13**.

The temperature contour's iteration step is 100 steps. Among them, frames 1–11, 20, 30, 40, 50, 60, 80, and 100 are shown in **Figure 11**, which shows the whole process of natural convection temperature changes', and the dynamics are more vivid and intuitive.

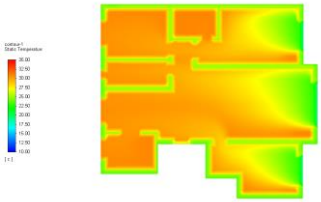

(a) Temperature contour at t = 1 s

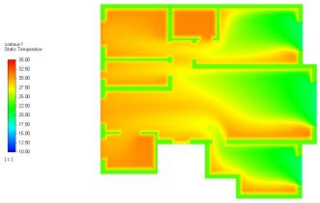

(b) Temperature contour at t = 2 s

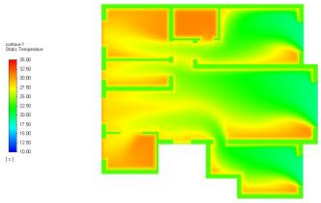

(c) Temperature contour at t = 3 s

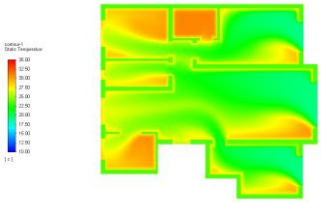

(d) Temperature contour at t = 4 s

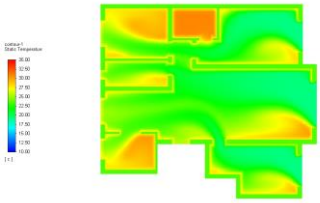

(e) Temperature contour at t = 5 s

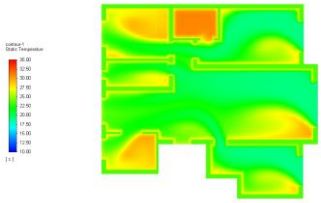

(f) Temperature contour at t = 6 s

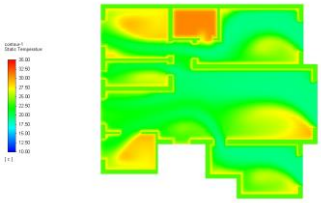

(g) Temperature contour at t = 7 s

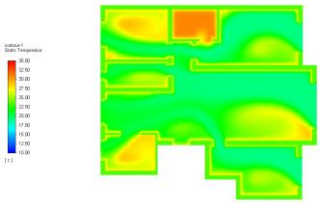

(h) Temperature contour at t = 8 s

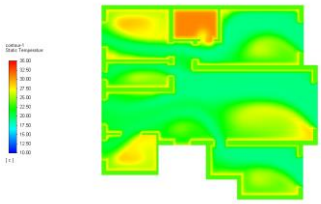

(i) Temperature contour at t = 9 s

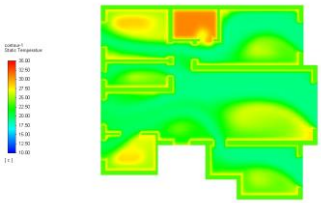

(j) Temperature contour at t = 10 s

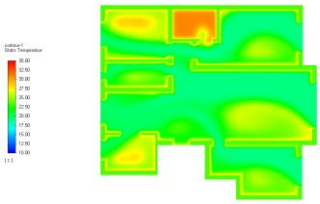

(k) Temperature contour at t = 11 s

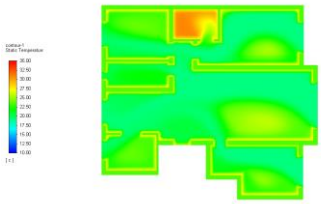

(l) Temperature contour at t = 20 s

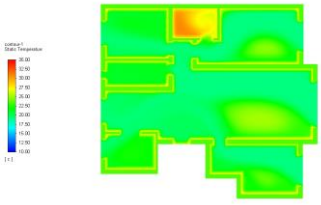

(m) Temperature contour at t = 30 s

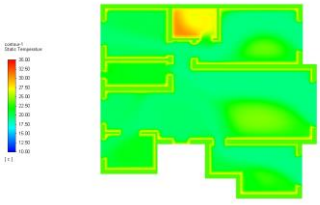

(n) Temperature contour at t = 40 s

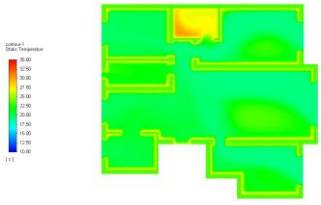

(o) Temperature contour at t = 50 s

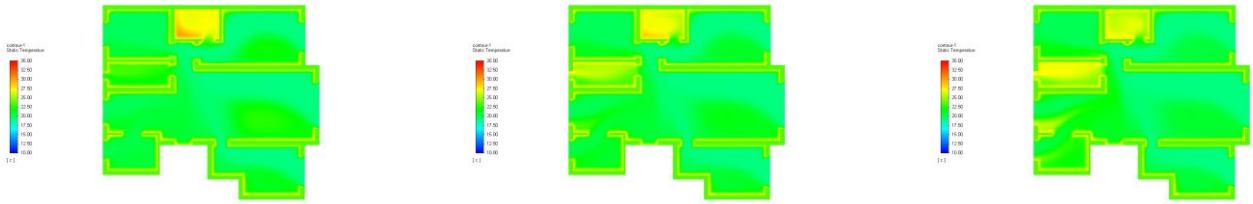

(p) Temperature contour at t = 60 s **(q)** Temperature contour at t = 80 s **(r)** Temperature contour at t = 100 s

Figure 11. Temperature contour at different times under working condition 2.

As can be seen from **Figure 11**, when T = 1 s to T = 9 s, rooms *A* and *C* can meet the human body's temperature requirements only by natural ventilation. When T = 10 s to T = 20 s, room *B* can also reach a comfortable temperature by natural ventilation. It can be seen that the room close to the air inlet can quickly achieve human thermal comfort. When T = 21 s to T = 60 s, *H* room's temperature is high, and when the ventilation time is insufficient, mechanical ventilation combined with natural ventilation can be used for room *F*, which is conducive to better energy saving and meets people's temperature comfort requirements. When T = 61 s to T = 100 s, when the natural ventilation's time reaches the duration, only natural ventilation can make all the rooms (*A*, *B*, *C*, *D*, *E*, *F*, *G* and *H* rooms) reach the human body's comfortable temperature.

A trace diagram of particle pathlines of working condition 2 is shown in **Figure 12**.

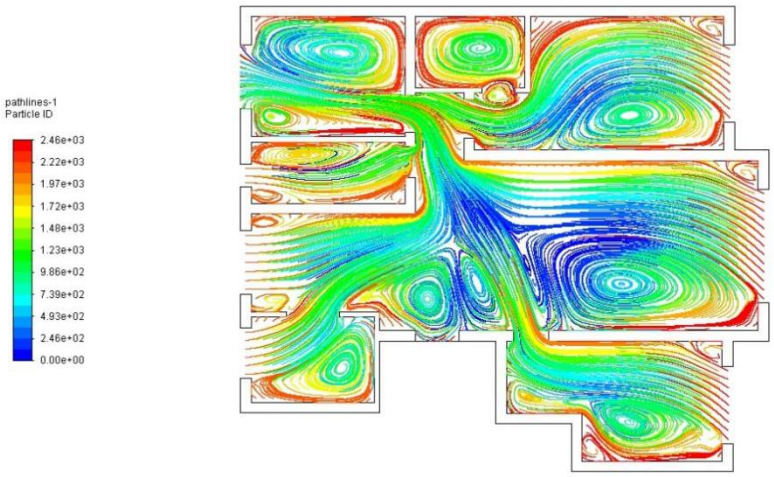

Figure 12. Trace diagram of particle pathlines of working condition 2.

By comparing **Figures 10** and **12**, it can be seen that vortices' are generated by a 45° upward and 45° downward inlet wind projection angle.

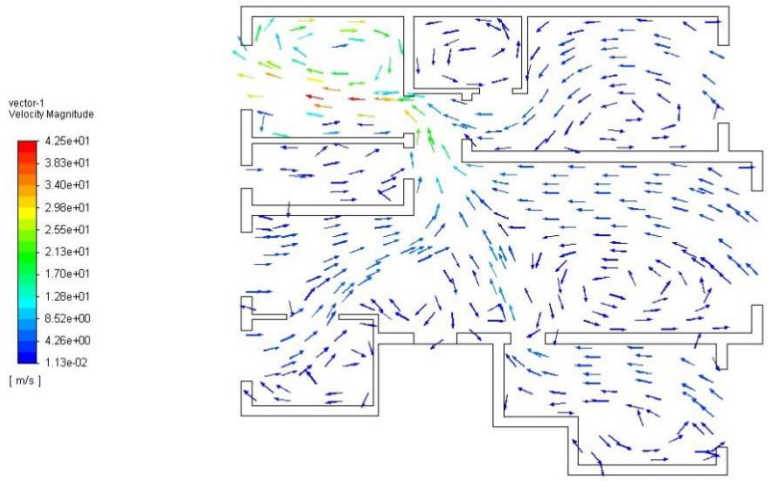

Figure 13. Velocity vector diagram.

Compared with the velocity vector diagram in **Figure 5**, the flow velocity is located in about the same position, which can be analyzed with reference to **Figure 5**.

As can be seen from **Table 3**, by comparing the wind's magnitude and direction angles, the trace diagram's eddy distribution rule can be obtained by comparing and analyzing. At the same time, it can be concluded that when the wind direction projection angle is 45°, the ventilation effect can be effectively improved.

Table 3. Comparative analysis of projection angles of different wind directions.

(1) 0°	**(2) Oblique down 30°**	**(3) Oblique upward 30°**	**(4) Oblique down 45°**	**(5) Oblique upward 45°**	**(6) Oblique down 60°**	**(7) Oblique upward 60°**
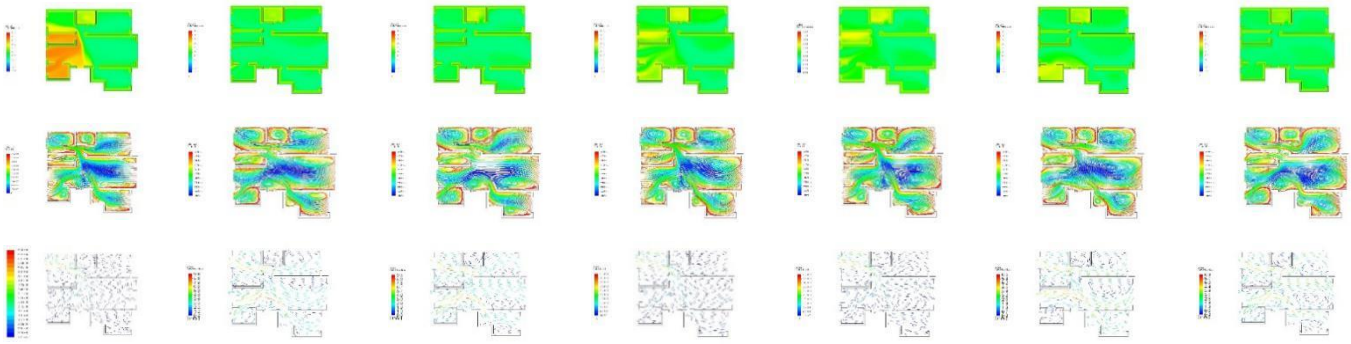						

(4) Indoor field of working condition 4

The temperature contour of working condition 4 is shown in **Figure 14**, the velocity vector diagram of working condition 4 is shown in **Figure 15**, and the trace diagram of working condition 4 is shown in **Figure 16**.

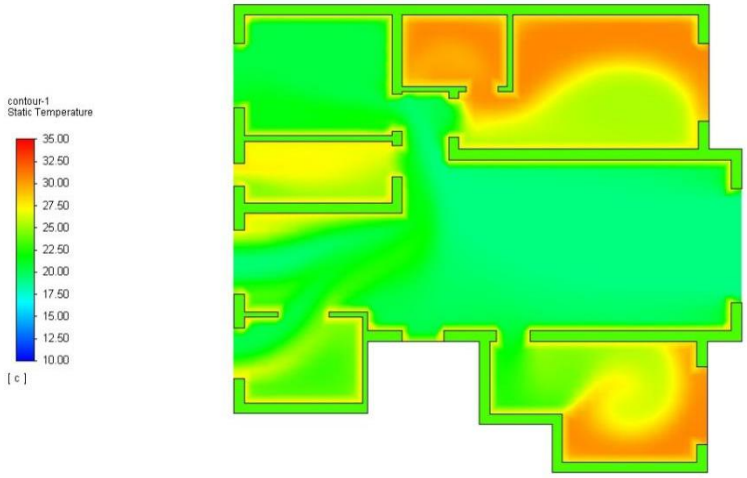

Figure 14. Temperature contour of working condition 4.

From **Figure 14**, it can be seen that only open the window 1, and *A*, *C* rooms are not well ventilated, and their energy savings are not as good as the window opening method and the inlet wind speed angle in **Figure 8**.

Wind deflectors can be set at the poorly ventilated room's door, so that better ventilation can be achieved and the human body's thermal comfort can be better met. At the same time, it can be concluded that when the inlet and outlet areas are equal, the opening area is larger, the more air enters the room. What's more, when the air outlet area is larger than the air inlet area, it is more beneficial to indoor natural ventilation.

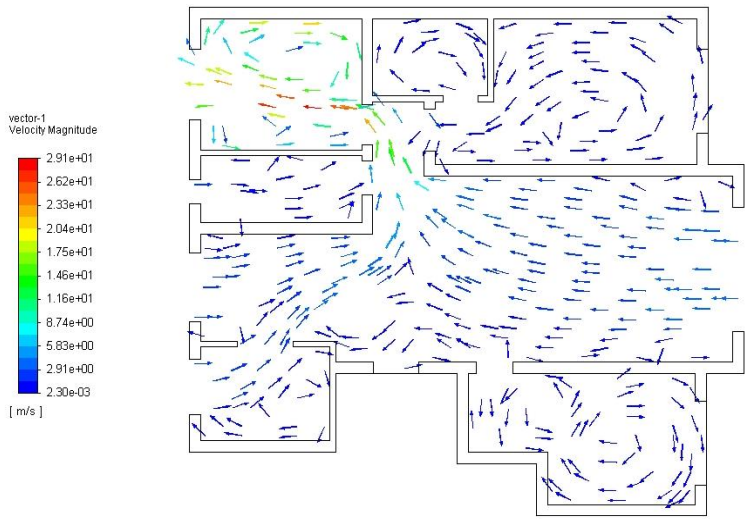

Figure 15. Indoor velocity vector diagram of working condition 4.

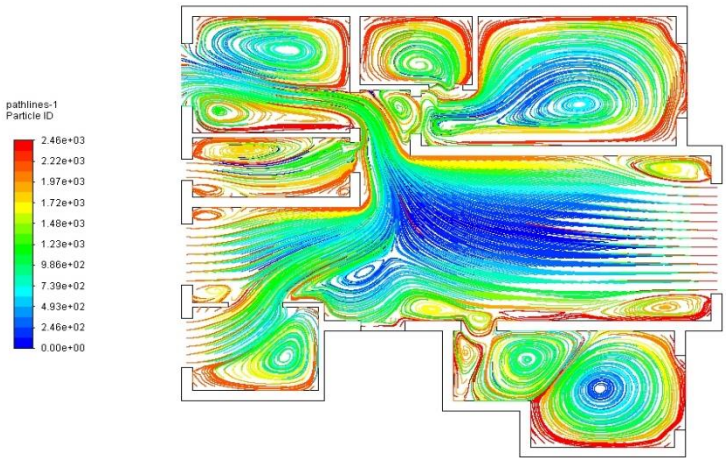

Figure 16. Trace diagram of working condition 4.

By comparing the traces of **Figures 7** and **16**, it can be seen that the rooms without windows (*A* and *C* rooms) generate large vortices, which is not conducive to the room's cleanliness requirements. That is to say, when the air inlet's area is larger, the airflow range is more uniform. At the same time, it can be inferred that the location and the room opening's area determine whether a certain air flow rate can be obtained in the room and whether the indoor flow field is uniform.

(5) Indoor flow field of working condition 5

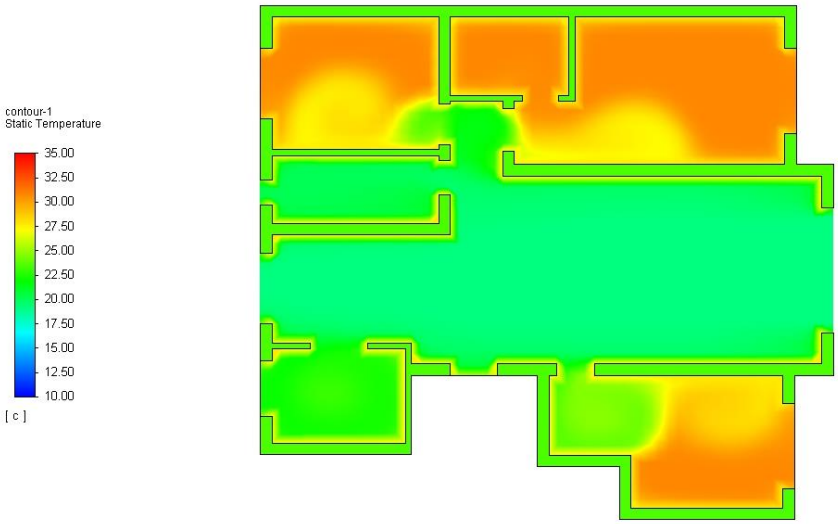

Figure 17. Temperature contour of working condition 5.

Through **Figure 17**, it can be seen that in the direct airflow zone, such as *B*, *E*, and *F* rooms, they can better reach the human body's thermal comfort temperature, while the room temperature, which is without open windows, such as in *A*, *C*, *D* and H rooms', is higher.

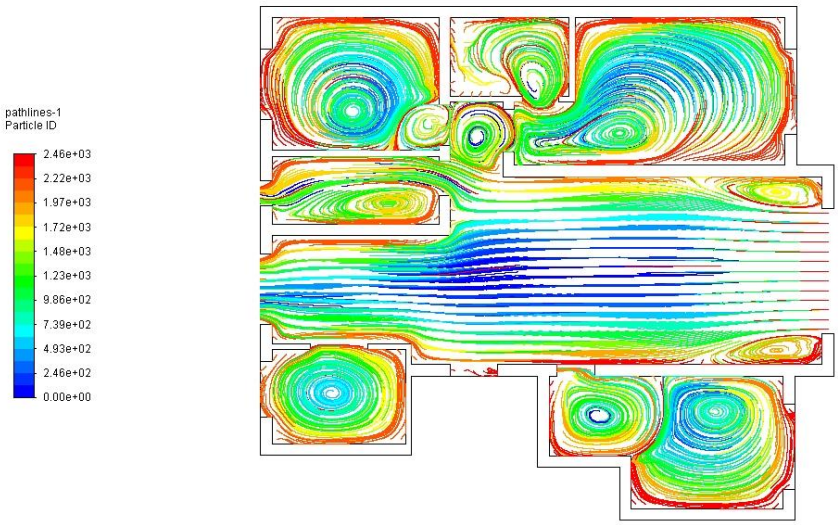

Figure 18. Trace diagram of working condition 5.

As can be seen from **Figure 18**, the opening position is set in the center, the airflow is straight, and the convective field is evenly distributed. What's more, it can be seen that there is almost no vortex in the direct airflow zone, which is conducive to indoor cleanliness.

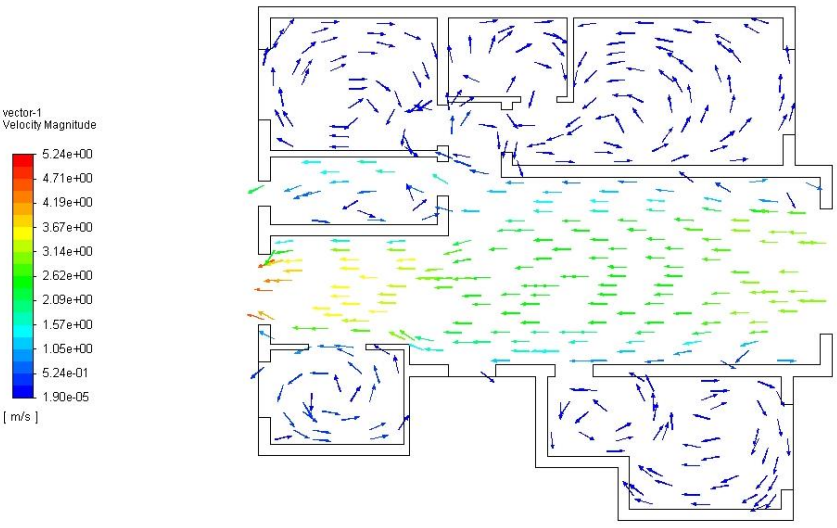

Figure 19. Velocity vector diagram of working condition 5.

Through **Figure 19**, it can be seen that the airflow through the area has a large flow velocity due to the lack of obstacles, which is conducive to human body heat dissipation. In the area blocked by obstacles, due to the small air inflow and low flow velocity, it is not conducive to the human body's heat dissipation under indoor high-temperature conditions.

(6) Indoor flow field of working condition 6

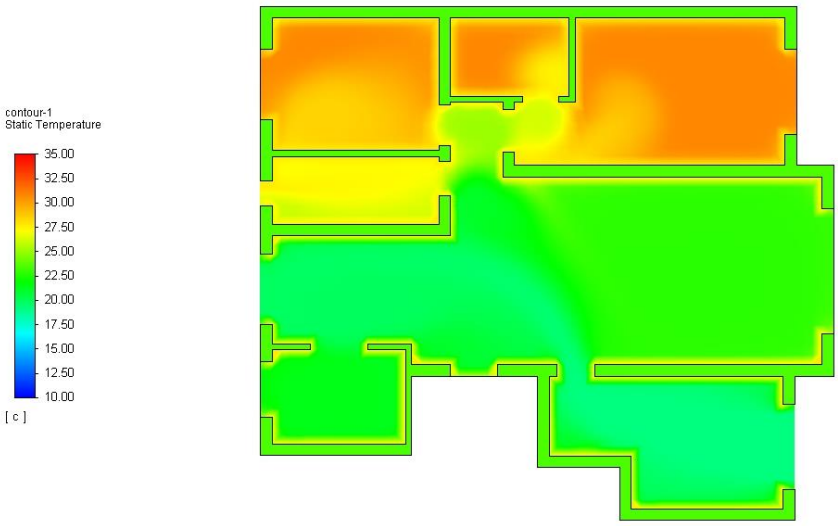

Figure 20. Temperature contour of working condition 6.

It can be seen from **Figure 20** that the room's indoor temperature without open windows is high, and it needs to be combined with mechanical equipment to refrigerate in order to better achieve the human's comfortable temperature.

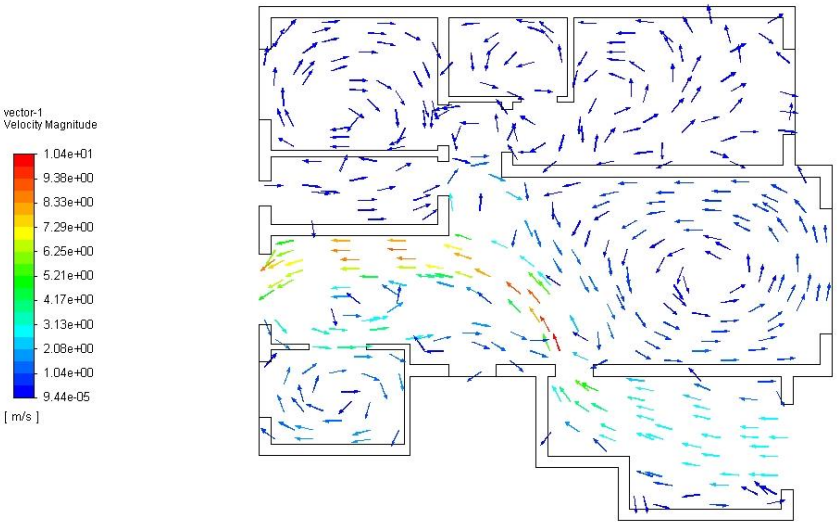

Figure 21. Velocity vector diagram of working condition 6.

Figure 21 shows that the airflow velocity along the opening and outlet area is high, which is conducive to indoor ventilation. Around the un-windowed rooms, there is almost no airflow.

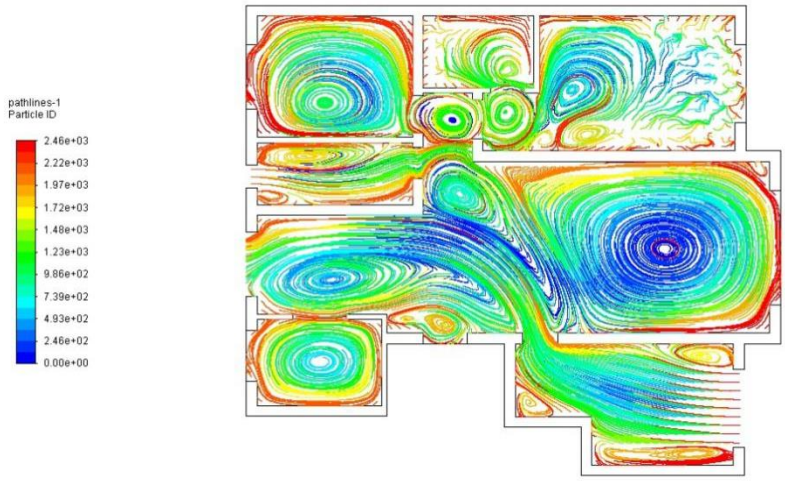

Figure 22. Trace diagram of working condition 6.

From **Figure 22**, it can be seen that there is almost no airflow in A room, and the indoor ventilation effect is not achieved. At the same time, it can be seen that the opening is set on one side, which can produce more vortices so that the flow field is unevenly distributed, and then affect the cleanliness of the room and people's requirements for indoor cleanliness.

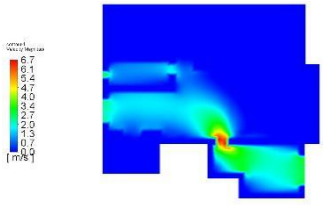

(a) Velocity contour at t = 1 s

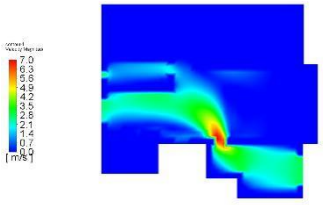

(b) Velocity contour at t = 2 s

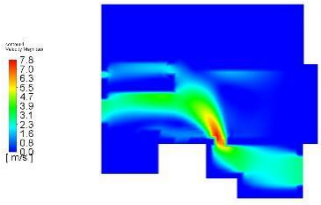

(c) Velocity contour at t = 3s

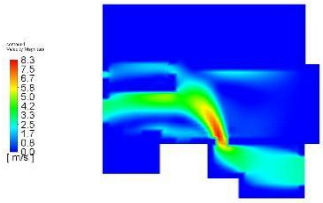

(d) Velocity contour at t = 4 s

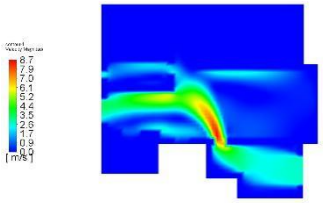

(e) Velocity contour at t = 5 s

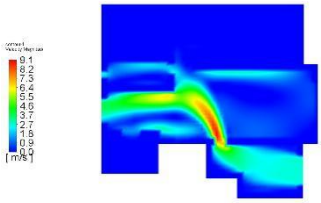

(f) Velocity contour at t = 6 s

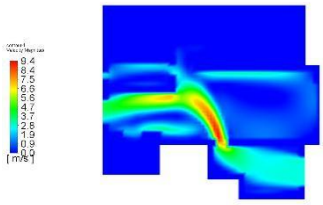

(g) Velocity contour at t = 7 s

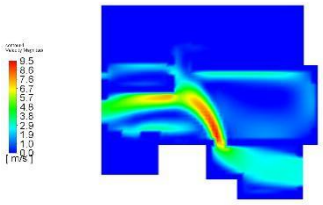

(h) Velocity contour at t = 8 s

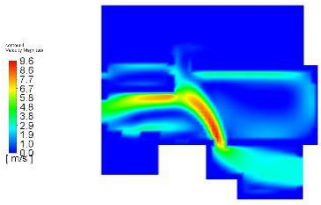

(i) Velocity contour at t = 9 s

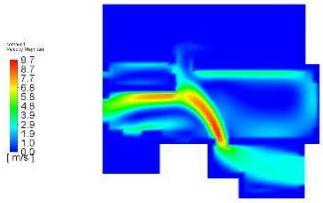

(j) Velocity contour at t = 10 s

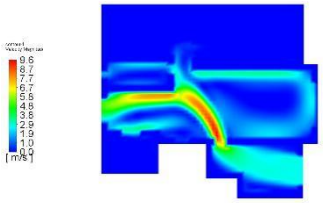

(k) Velocity contour at t = 11 s

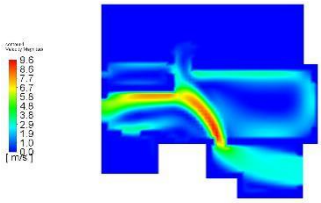

(l) Velocity contour at t = 12 s

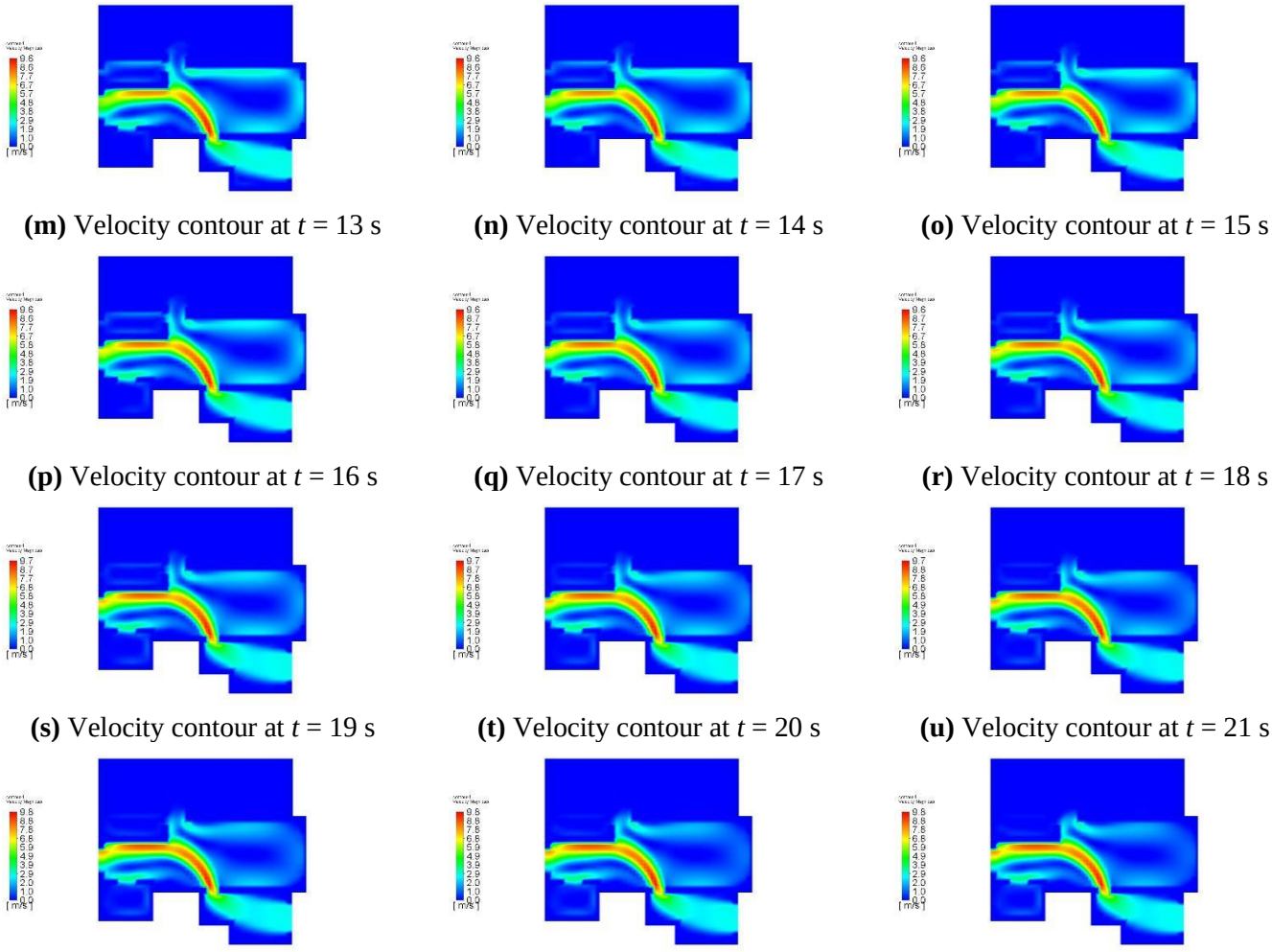

(m) Velocity contour at t = 13 s **(n)** Velocity contour at t = 14 s **(o)** Velocity contour at t = 15 s

(p) Velocity contour at t = 16 s **(q)** Velocity contour at t = 17 s **(r)** Velocity contour at t = 18 s

(s) Velocity contour at t = 19 s **(t)** Velocity contour at t = 20 s **(u)** Velocity contour at t = 21 s

(v) Velocity contour at t = 22 s **(w)** Velocity contour at t = 23 s **(x)** Velocity contour at t = 24 s

Figure 23. Velocity contour at different times under working condition 6.

It can be seen from the velocity contours at different times in **Figure 23**. When T = 1 s, the wind speed in room C is the largest, and the room C door's wind speed is the largest, and the maximum instantaneous wind speed can reach 6.7 m/s. When T = 2 s to T = 18 s, room C's maximum instantaneous flow velocity gradually increases from 7.0 m/s to 9.6 m/s due to the door's small opening and the large inlet wind speed. When T = 19 to T = 21 s, the wind speed of the area from C room's door to F room is high, and the maximum instantaneous wind speed can reach 9.7 m/s. When T = 22 to T = 24 s, the maximum instantaneous wind speed can reach 9.8 m/s. It can be seen that the room's structural design can greatly affect the wind speed's value, and then affect the human body's comfort about the velocity.

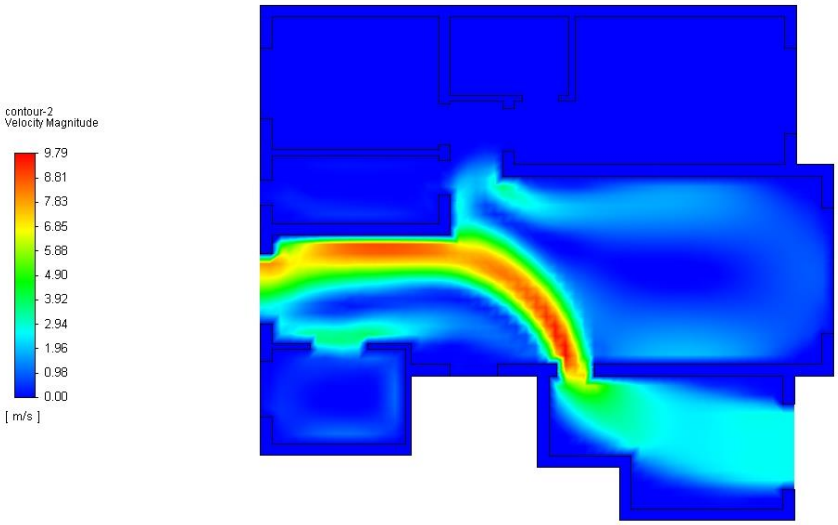

Figure 24. Final state of velocity contour under working condition 6.

From the final state of the velocity contour under working condition 6 in **Figure 24**, it can be seen that the air circulation area's wind speed value is quite high. Wind speed in the area through which inlet wind flows is higher, and wind speed is higher in the area where the wind speed is concentrated in the area from the entrance of room *C* to room *F*. In summer, when ventilation does not significantly lower indoor temperature, air speed becomes a main factor for cooling [19]. Higher wind speeds increase ventilation and the air change ratio of a building, thereby lowering the inside temperature of the building [20]. What's more, air velocity affects the thermal comfort of the human body by affecting convective heat transfer and air evaporation [21].

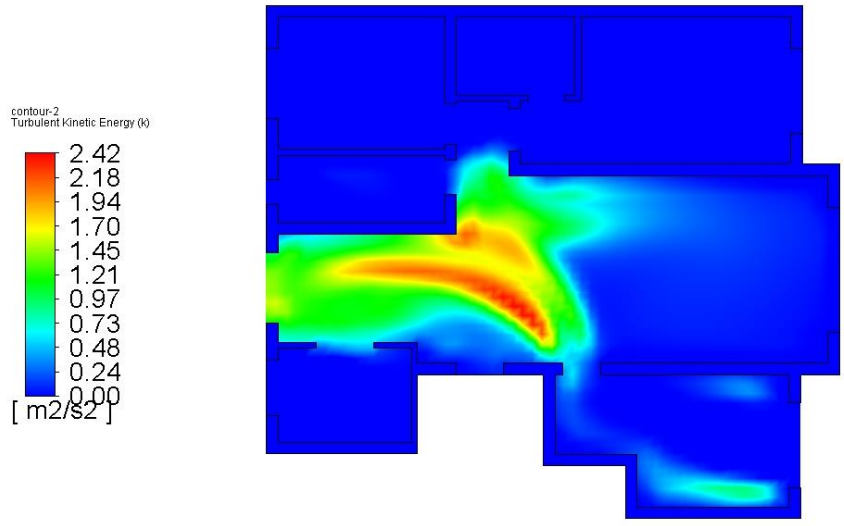

Figure 25. Final state of turbulent kinetic energy contour under working condition 6.

As can be seen from **Figure 25**, when the velocity value changes abruptly, the turbulent kinetic energy is larger, and the higher turbulent kinetic energy value is concentrated in room *F*. It can be seen that when wind speed changes abruptly, the turbulent kinetic energy is large, which makes the indoor airflow distribution uneven.

Therefore, the window's opening position can also affect people's speed comfort requirements.

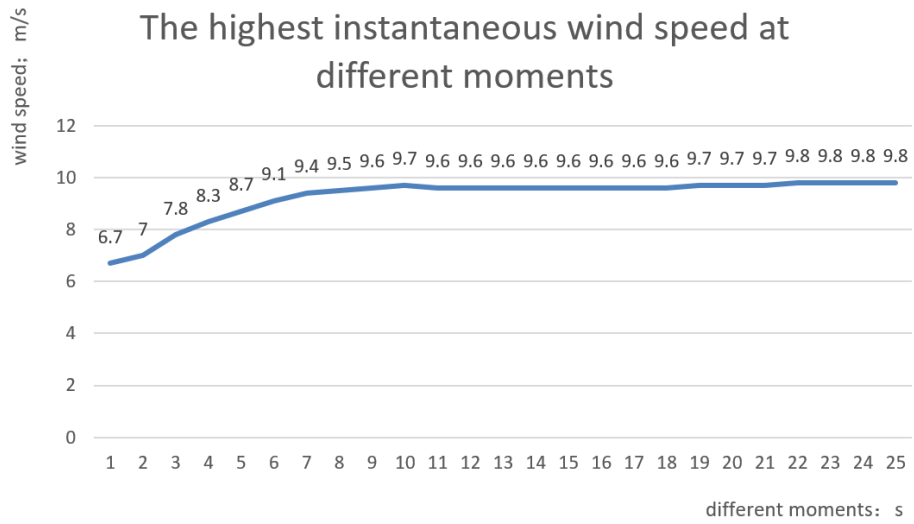

Figure 26. The highest instantaneous wind speed at different moments.

It can be seen from **Figure 26**. After T = 19 s, as the ventilation time increases, the maximum instantaneous wind speed value tends to be balanced. Through this line chart, wind speed value's change trend at different times can be vividly and intuitively analyzed. Thereby, it can better analyze indoor wind speed's value impact on human comfort.

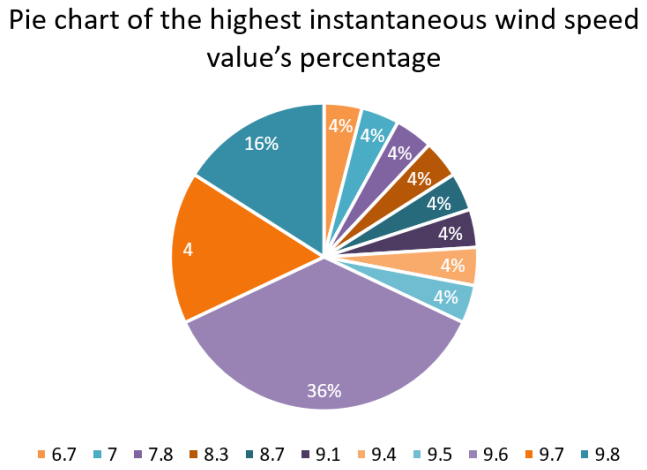

Figure 27. Pie chart of the highest instantaneous wind speed value's percentage.

As can be seen from **Figure 27**, it can be intuitively analyzed that the highest instantaneous wind speed of 9.6 m/s accounts for the largest proportion. Followed by 9.7 m/s and 9.8 m/s, accounting for 16%. The remaining wind speed's value accounts for 4%.

5. Discussion

Through the above flow field analysis, it can be seen that indoor temperature has a huge impact on people's comfort, so the author summarizes the temperature regions'

percentage from working conditions 1 to 6, which is helpful to intuitively analyze the temperature area that can reach human thermal comfort, and the proportion distribution figure is shown in **Figure 28**.

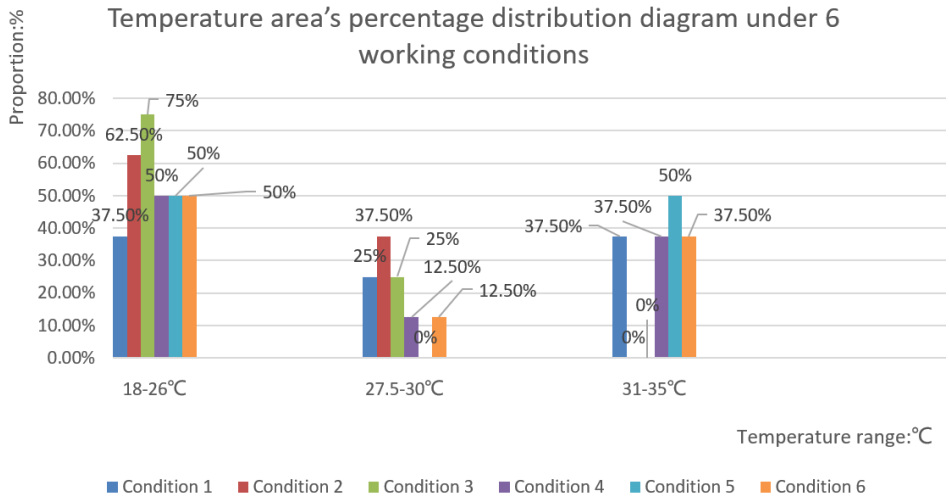

Figure 28. Temperature area's percentage distribution diagram under 6 working conditions.

It can be seen from **Figure 28** that under working condition 1, the three rooms of *A*, *B* and *C* can reach the human body's thermal comfort temperature through natural ventilation. Among them, the number of rooms that can reach the human thermal comfort's comfortable temperature (18 ℃–26 ℃) accounts for 37.5% of the rooms' total number.

What's more, under working condition 2, the five rooms of *A*, *B*, *C*, *D* and *E* can reach the human body's thermal comfort temperature through natural ventilation. Among them, the number of rooms that can reach the human thermal comfort's comfortable temperature (18 ℃–26 ℃) accounts for 62.5% of the rooms' total number.

Meanwhile, under working condition 3, the six rooms of *A*, *B*, *C*, *D*, *F* and *G* can reach the human body's thermal comfort temperature through natural ventilation. Among them, the number of rooms that can reach the human thermal comfort's comfortable temperature (18 ℃–26 ℃) accounts for 75% of the rooms' total number.

At the same time, condition 4 includes *BDFG* four rooms can reach thermal comfort temperature, condition 5 includes *BEFG* four rooms can reach thermal comfort temperature, and condition 6 includes *BCFG* four rooms can reach thermal comfort temperature, each accounting for 50%.

Therefore, when the above-mentioned room temperature is in the range of 18 ℃–26 ℃, the room can be cooled only by natural ventilation, and when the room temperature reaches the range of 31 ℃–35 ℃, the mechanical ventilation mode and the natural ventilation mode can be combined, which is not only conducive to the building's energy saving but also better satisfies the human body's thermal comfort. The combination of mechanical ventilation and natural ventilation is not only beneficial for building energy conservation, but also better meets the thermal comfort of the human body. This indicates that when designing and operating building

ventilation systems, energy efficiency and comfort should be comprehensively considered to seek the optimal balance point. Dynamically adjusting ventilation strategies based on changes in room temperature (such as transitioning from pure natural ventilation to combined mechanical ventilation) is an effective means of improving indoor environmental quality and energy efficiency. This emphasizes the importance of flexibly adjusting ventilation methods according to specific situations in practical applications.

6. Conclusion

Natural ventilation shows high application potential in buildings because of its highly efficient indoor environment quality improvement and building energy-saving expectations. In this research, taking a practical new construction project of a home interior architecture, located in Liaoning, China, as an example, detailed architecture and structure design are conducted and optimized with natural ventilation considerations under local climatic conditions. Based on simulation, results show that building interior architectural design is favorable for natural ventilation. Therefore, this typical case offers a design means for interior buildings to increase indoor thermal comfort and lower building energy consumption. Conclusions are listed as follows:

(1) From the comparison of boundary conditions 1 and 2, it can be seen that when organizing natural ventilation, the window orientation is inclined to about 45°from the dominant wind direction in summer, which can cause air turbulence in the room to move in a circular motion along the surrounding of the room, thereby increasing the air flow rate at the side walls and corners and improving the ventilation effect. At the same time, from the temperature contour's comparison of boundary condition 1 and boundary condition 2, it can be seen that the air inlet angle of 45°can better reach the human body's thermal comfort temperature: 18 ℃–26 ℃. Therefore, increasing the opening angle to about 45° can effectively improve the ventilation effect. Use ventilation structures such as wind deflectors, floor-to-ceiling windows, openwork walls and folding doors to facilitate natural ventilation. As can be seen in the geometric 3D model, this case model includes a floor-to-ceiling window, which is better for ventilation.

(2) From the comparison of boundary conditions 1 and 4, it can be seen that the larger the inlet area, the more uniform the air flow range. Meanwhile, when the air outlet's area is larger than the air inlet area, it is more beneficial to indoor ventilation. It can also be concluded that the window opening's position determines the flow field's distribution in the room. The opening position is located in the center, and the direct airflow is evenly distributed in the convective field. But when the opening is on one side, it is easy to shift the airflow, resulting in a vortex in some areas, thus it is not conducive to indoor cleanliness. At the same time, the opening distance should not be too close, if the distance is too close, the air can be directed to one side, and it is easier to generate vortices.

Research results can provide theoretical guidance on how to effectively utilize natural ventilation to improve indoor air quality. This not only helps to reduce indoor pollutant concentrations, but also provides fresh and healthy air, which has a positive impact on the health and quality of life of residents. Research results are also beneficial

for optimizing indoor design, achieving efficient natural ventilation, and providing practical and feasible solutions for building energy conservation. This research not only has important theoretical value, but also provides useful guidance and inspiration for architectural design practice, building energy efficiency, green building development, and improving resident satisfaction.

Author contributions: Conceptualization, YF and BZ; methodology, YF; software, YF; validation, YF; formal analysis, YF; investigation, YF; resources, YF; data curation, YF; writing—original draft preparation, YF; writing—review and editing, YF; visualization, YF; supervision, BZ; project administration, YF; funding acquisition, YF. All authors have read and agreed to the published version of the manuscript.

Institutional review board statement: Not applicable.

Informed consent statement: Not applicable.

Conflict of interest: The authors declare no conflict of interest.

References

1. Weber RE, Mueller C, Reinhart C. A hypergraph model shows the carbon reduction potential of effective space use in housing. Nature Communications. 2024; 15(1). doi: 10.1038/s41467-024-52506-z
2. Li W, Xu X, Yao J, et al. Natural ventilation cooling effectiveness classification for building design addressing climate characteristics. Scientific Reports. 2024; 14(1). doi: 10.1038/s41598-024-66684-9
3. Chen H, Ding X, Li R, et al. An experimental case study of natural ventilation effects on the residential thermal environment and predicted thermal comfort in Kunming. Case Studies in Thermal Engineering. 2024; 56: 104198. doi: 10.1016/j.csite.2024.104198
4. Chen Y, Luo L. Energy consumption behaviors and the potential of natural ventilation emission reduction in residential building. Journal of Asian Architecture and Building Engineering. 2023; 23(6): 2029-2040. doi: 10.1080/13467581.2023.2278471
5. Hsu HC, Chang CW, Chen CC, et al. Natural Ventilation: Optimizing Window Opening Size for CO2 Concentration Control and Thermal Comfort on Nonwindward Facades. Indoor Air. 2024; 2024(1). doi: 10.1155/2024/1435400
6. Zhang M, Han W, He Y, et al. Natural Ventilation for Cooling Energy Saving: Typical Case of Public Building Design Optimization in Guangzhou, China. Applied sciences. 2024; 14(2): 610. doi: 10.3390/app14020610
7. Iskandar L, Bay-Sahin E, Martinez-Molina A, et al. Evaluation of passive cooling through natural ventilation strategies in historic residential buildings using CFD simulations. Energy and Buildings. 2024; 308: 114005. doi: 10.1016/j.enbuild.2024.114005
8. Kocik S, Psikuta A, Ferdyn-Grygierek J. Influence of window and door opening on office room environment and human thermal sensation during different seasons in moderate climate. Building and Environment. 2024; 259: 111669. doi: 10.1016/j.buildenv.2024.111669
9. Cheng Y, Xie S, Yang M, et al. A study on natural ventilation of dormitories for college students in northeast China during spring: A case of linear-shaped dormitory buildings. Journal of Building Engineering. 2024; 90: 109402. doi: 10.1016/j.jobe.2024.109402
10. Nguyen VT, Boppana B, Leong J, et al. Analysis and assessment of natural ventilation in the design of urban precincts using an overset grid CFD approach. Building and Environment. 2025; 269: 112352. doi: 10.1016/j.buildenv.2024.112352
11. Wang C, Jin M, Cheng H. Influence of deflectors on indoor airflow velocity distribution under natural ventilation conditions. Frontiers in Energy Research. 2024; 12. doi: 10.3389/fenrg.2024.1327577
12. Nasrollahi N, Ghobadi P. Field measurement and numerical investigation of natural cross-ventilation in high-rise buildings; Thermal comfort analysis. Applied Thermal Engineering. 2022; 211:118500. doi: 10.1016/j.applthermaleng.2022.118500

13. Tian L, Liu ZA, Li Y, et al. Influence and optimization of building opening configurations on the performance of enhanced roof ventilation units (ERU): a numerical and orthogonal study. Case Studies in Thermal Engineering. 2025; 66: 105753. doi: 10.1016/j.csite.2025.105753
14. Zhang C, Wen CY, Jia Y, et al. Enhancing the accuracy of physics-informed neural networks for indoor airflow simulation with experimental data and Reynolds-averaged Navier–Stokes turbulence model. Physics of Fluids. 2024; 36(6). doi: 10.1063/5.0216394
15. Serra N. Revisiting RANS turbulence modelling used in built-environment CFD simulations. Building and Environment. 2023; 237: 110333. doi: 10.1016/j.buildenv.2023.110333
16. Zhang T, Zhou H, Wang S. An adjustment to the standard temperature wall function for CFD modeling of indoor convective heat transfer. Building and Environment. 2013; 68: 159-169. doi: 10.1016/j.buildenv.2013.06.009
17. Liu F, Li Y, Wang Y, et al. A Numerical Investigation of the Thermal Performance of a Gabion Building Envelope in Cold Regions with a Mountainous Climate. Applied Sciences. 2023; 13(15): 8809. doi: 10.3390/app13158809
18. Polanco JI, Müller NP, Krstulovic G. Vortex clustering, polarisation and circulation intermittency in classical and quantum turbulence. Nature Communications. 2021; 12(1). doi: 10.1038/s41467-021-27382-6
19. Li R, Liu J, Chen X, et al. Transient thermal comfort during summer in air-conditioned indoor and naturally ventilated transitional spaces − A field study in Zhengzhou, China. Energy and Buildings. 2025; 328: 115122. doi: 10.1016/j.enbuild.2024.115122
20. Staffell I, Pfenninger S, Johnson N. A global model of hourly space heating and cooling demand at multiple spatial scales. Nature Energy. 2023; 8(12): 1328-1344. doi: 10.1038/s41560-023-01341-5
21. Fu Y, Zhao B. Research progress on thermal comfort evaluation in vehicle cab. Mechanical Engineering Advances. 2025; 3(1): 2098. doi: 10.59400/mea2098